ChemPlusChem
Full Papers

ChemPubSoc Europe

DOI: 10.1002/cplu.201((will be completed by the editorial staff))

Nanodiamond-TiO_2 composites for heterogeneous photocatalysis

Luisa M. Pastrana-Martínez,[a] Sergio Morales-Torres,[a] Sónia A.C. Carabineiro,[a] Josephus G. Buijnsters,[b] Joaquim L. Faria,[a] José L. Figueiredo,[a] Adrián M.T. Silva*[a]

The present work is pioneer in the synthesis and application of composites based on micro- and nanodiamonds for the photocatalytic degradation of environmental water pollutants. Micro- and nanodiamond powders (with particle sizes of 1-3 μm and 2-10 nm, respectively) were combined with TiO_2, varying the carbon phase content and tested as composite photocatalysts for the degradation of diphenhydramine pharmaceutical water pollutant under near UV-Vis irradiation. These composites exhibited higher photocatalytic activity than the respective bare materials. In addition, composites prepared with pristine nanodiamonds were always more active than those prepared with microdiamonds at the same carbon content. A significant enhancement in the photocatalytic performance was observed when the composite was prepared with 15 wt.% of nanodiamonds oxidized in air at 703 K, these oxidized nanodiamonds containing mainly carboxylic anhydrides, lactones, phenols and, to a lower extent, carbonyl/quinone groups on their surface.

Introduction

Diamond has generated many theoretical and practical studies over the past few decades due to its specific properties such as wide bandgap, high carrier transport speed, thermal conductivity, optical transparency and superior hardness.[1] Microdiamonds (MDs) are commonly defined as diamond powders with particle size smaller than 500 μm. They can be extracted from natural rocks at very affordable costs, having a low value in the market and, therefore, being potential precursors of low-cost catalysts.

Obviously, nanodiamonds (NDs) have smaller particle size (typically 4-5 nm) than MDs and are rapidly becoming one of the most widely studied nanomaterials, since diamonds on the nanoscale have a higher surface area than MDs (BET surface areas around 300 $m^2\ g^{-1}$ for NDs, in contrast to 5 $m^2\ g^{-1}$ for MDs) which helps to create more reactive chemical surface groups.[2] With the development of new environmental friendly purification techniques, NDs are nowadays produced in large volumes at a low cost, which has stimulated immense interest in the fabrication of many novel products, including catalysts,[3] composites,[4] and magnetic sensors.[5] They have also been considered for medical applications (such as biomedical imaging and drug delivery) because nano-sized diamond particles were found less toxic than other carbon nanoparticles.[2b]

[a] *Dr. L.M. Pastrana-Martínez, Dr. S. Morales-Torres, Dr. S.A.C. Carabineiro, Prof. J.L. Faria, Prof. J.L. Figueiredo, Dr. A.M.T. Silva*
LCM – Laboratory of Catalysis and Materials – Associate Laboratory LSRE/LCM, Faculdade de Engenharia, Universidade do Porto
Rua Dr. Roberto Frias, 4200-465 Porto, Portugal
Fax: +351-22-5081449; Tel: +351-22-5081582
E-mail: adrian@fe.up.pt
[b] *Dr. J.G. Buijnsters*
Department of Metallurgy and Materials Engineering, KU Leuven
Kasteelpark Arenberg 44, B-3001 Leuven, Belgium

On the other hand, the photocatalytic activity of TiO_2 has been amply demonstrated for degradation of liquid and gas phase pollutants, water photolysis and carbon dioxide reduction.[6] Recently, graphene, the planar form of sp^2 hybridized carbon, and its derivatives, such as graphene oxide, have been efficiently used towards the development of photocatalysts when combined with TiO_2. In our recent publication,[7] dealing with diphenhydramine (DP) pharmaceutical and methyl orange dye as model pollutants, a significant enhancement of the photocatalytic activity was observed when graphene oxide was combined with TiO_2, this favourable effect being mainly attributed to the efficient interfacial electron transfer between the two constituent phases. In fact, it is well known that combination of TiO_2 with carbon materials, such as graphene oxide[7-8] and carbon nanotubes,[9] often results in composites with higher photocatalytic activity because issues relating to the low quantum yield and poor light-harvesting ability of TiO_2 are overcome.[10]

Considering all the above mentioned attractive properties of diamond, as well as the previous results obtained with composites based on graphene and its derivates, fine-grained diamond powders could be thought of as excellent candidates for photocatalytic applications when combined with TiO_2. To the best of our knowledge, there are no reports on the degradation of water pollutants by photocatalysis using composites prepared with TiO_2 and nano- (or micro-) diamonds. Only one publication was found reporting a gas-phase application of TiO_2 coated nanodiamond powder.[11] In such work, NDs-supported TiO_2 materials (synthetized by atomic layer deposition) were employed for the degradation of toluene under UV irradiation, 10% toluene degradation (and 5% conversion into CO_2) in steady state conditions being achieved.

Aiming at the development of innovative and highly efficient photocatalysts for the treatment of emergent and critical water

pollutants, the present work is focused on composites combining TiO_2 with MDs and NDs. These materials were tested under near UV-Vis irradiation and using DP pharmaceutical as model pollutant. The effect of the surface chemistry of the carbon phase on the photocatalytic efficiency of the resulting composite was studied, and the respective carbon content was optimized.

Results and Discussion

Scanning electron microscopy (SEM) and X-ray microanalysis (EDX)

Figure 1 shows SEM micrographs of representative studied materials (higher magnifications shown in insets). The bare TiO_2 agglomerated material prepared by the LPD method (Figure 1a) consists of anatase crystallites with an estimated size of 4-5 nm, determined by high resolution transmission electron microscopy (HRTEM) and selected area electron diffraction (SAED) in our previous publication.[7] Figure 1b illustrates a representative image of MDs, which consist of randomly oriented diamond grains (ca. 1-3 µm) with planar faces and sharp edges. Bare NDs (not shown) consist of primary particles with sizes in the range 2-10 nm, also determined by HRTEM in a previous publication,[12] the micro-scale morphology of NDs differing from that of MDs, as can be observed by comparing the SEM micrograph of the oxidized NDs (ND_{ox} in Figure 1c) and that obtained for MDs (Figure 1b). For ND_{ox}, the smaller nanoparticles form porous aggregates, in agreement with literature reporting the tendency of nanosized diamond particles to aggregate, in particular when they are functionalized, due to hydrogen bonding and van der Waals forces occurring between the particles.[13]

Regarding the composites, Figure 1d shows the micrograph of the composite prepared with 15 wt.% of pristine MDs (MDT-15), consisting of MDs embedded into TiO_2. A cross section of some of the composite particles is shown in Figure 1f, where it is confirmed that TiO_2 particles are grown around the MDs. This is corroborated by the respective EDX spectra (inset) recorded for zone 1 (corresponding to the inner phase, MDs – carbon) and zone 2 (corresponding to the outer phase, i.e. TiO_2 – Ti and O, as well as a small peak of F deriving from the TiO_2 precursor and of C from the vicinity containing the carbon phase). A similar morphology was observed for the other prepared composites (not shown), but composites prepared with NDs have smaller composite particles and the size of the respective TiO_2-NDs particles seems to be more homogeneous than the size of TiO_2-MDs particles. For instance, Figure 1e shows the particular case of ND_{ox}T-15 which consists of composite particles with smaller average size than in the case of MDT-15 (Figure 1d).

N_2 adsorption-desorption isotherms

The apparent surface area (S_{BET}), determined for the bare materials and for the composites prepared with 15 wt.% of carbon phase, are summarized in Table 1.

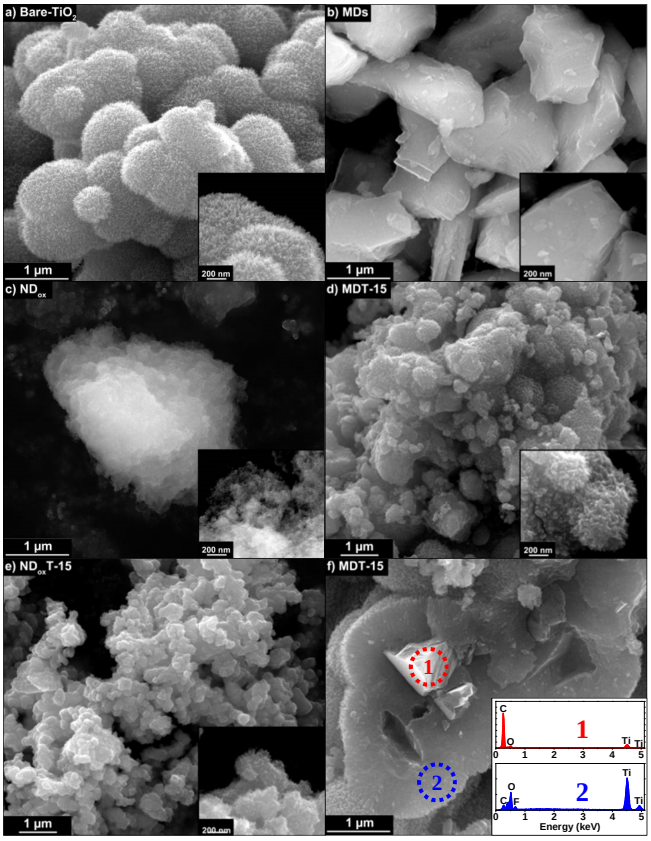

Figure 1. SEM micrographs of (a) Bare-TiO_2, (b) MDs, (c) ND_{ox}, (d) MDT-15, (e) ND_{ox}T-15 and (f) Aggregate and EDX spectra (inset) of MDT-15.

As expected, large differences were observed between the S_{BET} of MDs (< 5 m^2 g^{-1}) and NDs (295 m^2 g^{-1}), which are directly related with the different particle sizes of these materials. The oxidation treatment performed for NDs had a slight influence on their textural properties, the S_{BET} of ND_{ox} (253 m^2 g^{-1}) being lower than that of non-oxidized NDs (295 m^2 g^{-1}). This slight decrease in S_{BET} could be explained by the stronger aggregation of the nano-sized diamond particles when oxygenated surface groups are present.[13]

Table 1. Surface area (S_{BET}) determined for MDs, NDs, ND_{ox}, Bare-TiO_2 and for the composites prepared with 15 wt.% of carbon phase.

Catalyst	S_{BET} [m^2 g^{-1}]
MDs	< 5
NDs	295
ND_{ox}	253
Bare-TiO_2	118
MDT-15	75
NDT-15	74
ND_{ox}T-15	81

For all the composites containing 15 wt.% of diamond powder, comparable S_{BET} values were obtained (75, 74, 81 m^2 g^{-1} respectively for MDT-15, NDT-15 and ND_{ox}T-15). These values are similar regardless of the (i) nature (MDs or NDs), (ii) textural properties (e.g., S_{BET} < 5, 295 and 253 m^2 g^{-1} for MDs, NDs and ND_{ox}, respectively) and (iii) presence or absence of oxygenated surface groups (NDs and ND_{ox}) in the bare diamond powders. Therefore, these values indicate that the carbon phase is completely covered by TiO_2 particles and that those TiO_2 particles are arranged in a similar way on all these composites.

The adsorbed volume of N_2 for ND_{ox}T-15 was significantly smaller than that obtained for ND_{ox}, as well as the hysteresis loop of the isotherms (Figure 2). The average pore size distribution (PSD) obtained for the ND_{ox}T-15 composite was clearly different to that determined for ND_{ox} (inset of Figure 2). A mono-modal PSD with an average mesopore diameter of around 17.9 nm was observed for ND_{ox}, while for ND_{ox}T-15 the mesopores have sizes smaller than 6.0 nm. This different pore size distribution could justify the smaller adsorbed volume and surface area obtained in the case of ND_{ox}T-15, in comparison to that of ND_{ox}, resulting from the assembly of the TiO_2 particles onto the oxidized NDs. The N_2 adsorption isotherm of bare-TiO_2 is also presented in Figure 2. The isotherms and respective average pore size (< 2 nm) are relatively similar for bare-TiO_2 and ND_{ox}T-15, a larger adsorbed volume of N_2 at high relative pressure (indicative of wider pores) and a lower S_{BET} (Table 1) being obtained in the case of ND_{ox}T-15.

Temperature programmed desorption (TPD)

TPD technique was used for characterization of the surface functional groups of the NDs, before and after oxidative treatment with air at 703 K, and for the composite containing oxidized nanodiamonds (ND_{ox}T-15). The TPD spectra of evolved CO_2 and CO are shown in Figures 3a and 3b, respectively. The determined total amounts of CO_2 and CO as well as the respective percentage of molecular oxygen contents are collected in Table 2.

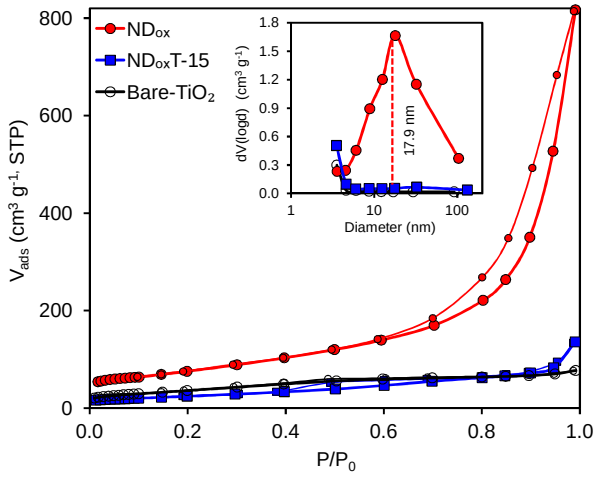

Figure 2. N_2 adsorption isotherms and pore size distribution (inset) for Bare-TiO_2, ND_{ox} and ND_{ox}T-15.

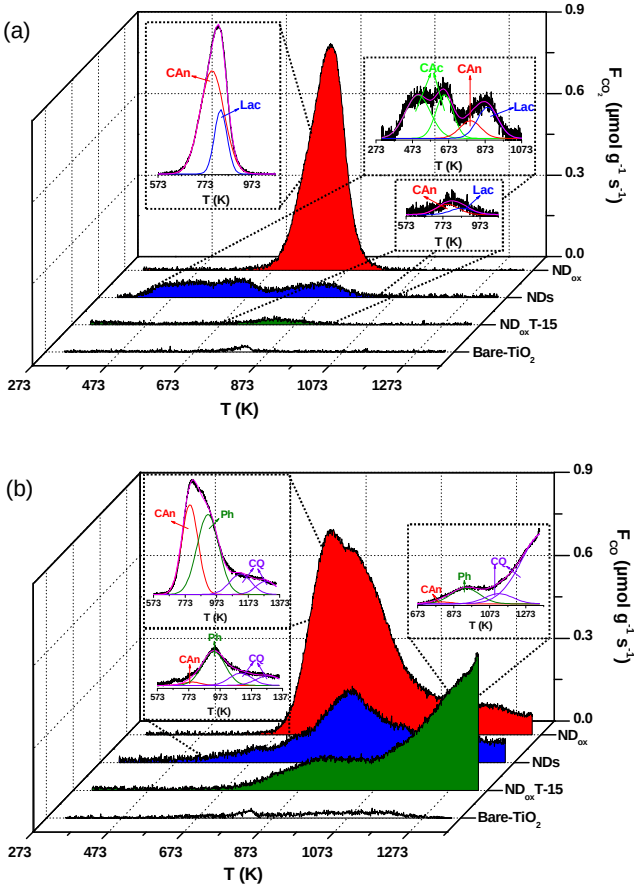

Figure 3. TPD profiles and their deconvolution using a multiple Gaussian function for ND_{ox}, NDs, ND_{ox}T-15 and Bare-TiO_2: (a) CO_2 evolution and (b) CO evolution.

For comparison, TPD spectra of bare-TiO_2 were also obtained (Figure 3) and, as expected, both evolved CO_2 and CO are negligible in this case. In addition, results obtained from deconvolution of the TPD spectra are compiled in Table 3, which includes (i) the temperature of the maximum, T_M, (ii) the width at half height, W, and (iii) the area, A, of all peaks. Carboxylic anhydrides decompose both as CO and CO_2 and, for this reason, the T_M, W and A values determined for CO_2 were maintained in the deconvolution of the TPD spectra related to CO, accordingly to the methodology reported in literature.[14]

Table 2. Amounts of CO_2 and CO releasing groups, and O_2 contents for NDs, ND_{ox} and ND_{ox}T-15.

Sample	CO_2 [μmol g^{-1}]	CO [μmol g^{-1}]	O_2 [wt.%]	CO/CO_2
NDs	295	845	2.3	2.9
ND_{ox}	1180	2400	7.6	2.0
ND_{ox}T-15	37	1160	2.0	31

Table 3. Results of the deconvolution of the TPD spectra taken from NDs, ND_{ox}, and ND_{ox}T-15.

	CO_2									CO								
	Carboxylic Acids (CAc)			Carboxylic Anhydrides (CAn)			Lactones (Lac)			Carboxylic Anhydrides (CAn)			Phenols (Ph)			Carbonyl/Quinones (CQ)		
	TM[a]	W[a]	A[b]	TM[a]	W[a]	A[b]	TM[a]	W[a]	A[b]	TM[a]	W[a]	A[b]	TM[a]	W[a]	A[b]	TM[a]	W[a]	A[b]
NDs	503 649	138 95	111 78	792	116	38	887	116	67	792	116	38	932	145	484	1105 1281	145 157	174 149
ND_{ox}	n.d.	n.d.	n.d.	804	103	891	841	54	290	804	103	891	919	138	1072	1124 1286	138 127	273 164
ND_{ox}T-15	n.d.	n.d.	n.d.	797	121	23	875	121	14	797	121	23	938	159	242	1124 1378	159 255	156 736

n.d. not detected
[a] (K). [b] (μmol g^{-1})

Regarding the pristine NDs, the amount of oxygen containing surface groups is relatively low (295 and 845 μmol g^{-1} for groups released as CO_2 and CO, respectively). The TPD spectrum of CO_2 (Figure 3a) can be decomposed into four peaks, two of them assigned to carboxylic acid groups (CAc) and related with strong (lower temperature/503 K) and weaker (higher temperature/649 K) carboxylic acids, and the two other peaks corresponding to carboxylic anhydrides/792-804 K (CAn) and lactones/841-887 K (Lac). On the other hand, the CO released (Figure 3b) is mainly attributed to carboxylic anhydrides (CAn), phenols (Ph) and carbonyl/quinone (CQ) groups decomposed at temperatures around 792-804, 919-938 and 1105-1124 K, respectively.[14] An additional peak placed at higher temperature, around 1281-1378 K, was also attributed to carbonyl/quinone (CQ) groups, but in this case located in different energetic sites.[14b, 15] A significant increase in the amount of the surface oxygen groups in the NDs is observed when the sample is oxidized when heated in air (i.e. ND_{ox}), the amount of CO_2 and CO released increasing respectively to 1180 and 2400 μmol g^{-1} (Figure 3 and Table 2).

For the oxidized sample, carboxylic acid groups were not observed because the oxidation treatment was carried out at a temperature (around 703 K) higher than that where decomposition of carboxylic acids occurs (around 503-649 K). Therefore, the amount of CO_2 is only related with the presence of carboxylic anhydrides (792-804 K) and lactones (841-887 K) while the amount of CO is due to carboxylic anhydrides (792-804 K), phenols (919-938 K) and carbonyl/quinone groups (1105-1378 K). As expected, a similar trend was found concerning the O_2 released from NDs and ND_{ox}, respectively 2.3 and 7.6 wt.% (Table 2), which is related to the increase in the total amount of oxygenated groups after the air treatment.

From the TPD spectra of ND_{ox} and ND_{ox}T-15, it can be concluded that the significant amount of oxygenated groups observed for ND_{ox} does not occur with the ND_{ox}T-15 composite. This fact can be related to the morphology of the composite, consisting of ND_{ox} completely embedded into TiO_2 (Figure 3), the TiO_2 phase protecting the oxidized nanodiamonds. Accordingly, the presence of TiO_2 onto ND_{ox} brings a decrease in the oxygen content (7.6% and 2.0% for ND_{ox} and ND_{ox}T-15, respectively) and the high CO/CO_2 ratio obtained (2.0 and 31 for ND_{ox} and ND_{ox}T-15, respectively) indicates that the amount of groups evolved as CO is larger than those evolved as CO_2 for the composite. However, the high contribution assigned to carbonyl/quinones (1105-1378 K) in the CO spectrum of the composite could be related to a delay on the release of other oxygenated groups due to the presence of TiO_2.

Photocatalytic experiments

Figures 4a, 4b and 4c depict the photocatalytic conversion of DP obtained for composites prepared with MDT, NDT, and ND_{ox}T, respectively, and different carbon contents. The results obtained for the prepared bare TiO_2 material and for the benchmark photocatalyst (P25) are also shown for comparison in Figure 4a.

The respective rate constants (*k*) were determined by application of the pseudo-first order kinetic model, according to Eq. 1:

$$[DP] = [DP]_0 \, e^{-k\,t} \qquad (1)$$

where [*DP*] corresponds to the DP concentration, *t* is the reaction time and $[DP]_0$ is the DP concentration at $t = 0$. The values of *k* were obtained by non-linear regression and the results are shown in Table 4.

It is important to refer that in such experiments the suspension was magnetically stirred for 30 min in dark to establish the adsorption-desorption equilibrium before turning on the lamp. The composites prepared with MDs, NDs and ND_{ox} always showed a low adsorption capacity (ca. 0.8-2.5% of DP) regardless of the content of diamonds.

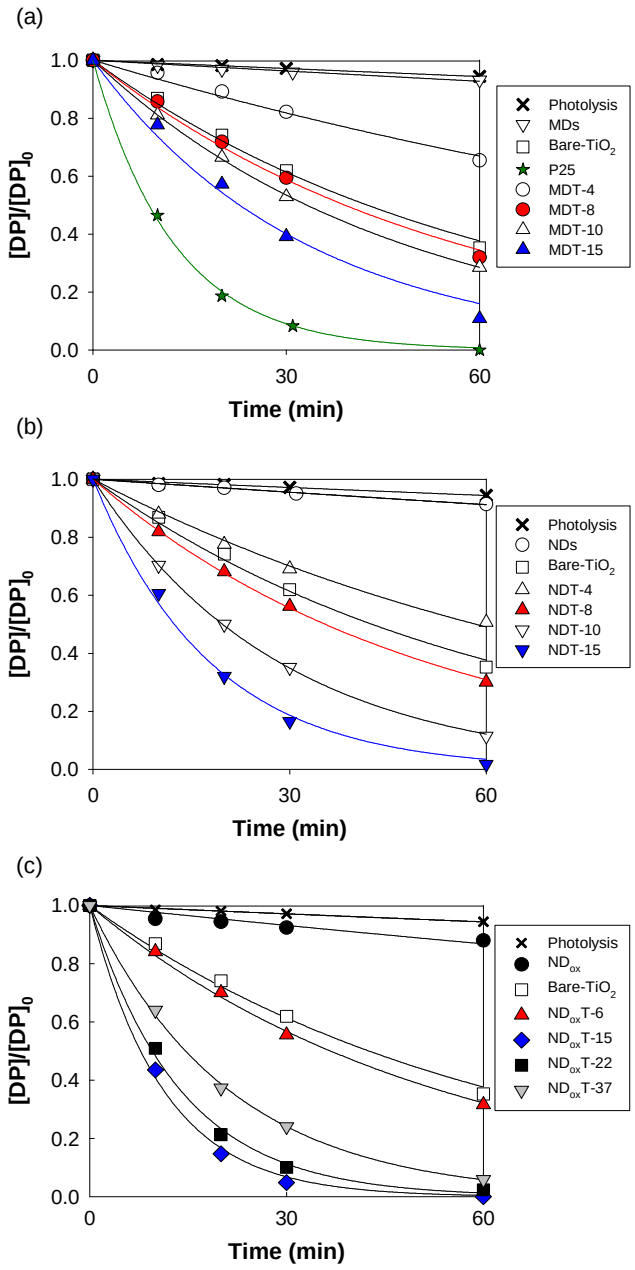

Figure 3. Normalized concentration of DP ($[DP]/[DP]_0$) under photocatalytic degradation with (a) MDs, Bare-TiO_2, P25 and TiO_2 composites with different contents of MDs; (b) NDs, Bare-TiO_2, and TiO_2 composites with different contents of NDs; (c) ND_{ox}, Bare-TiO_2, and TiO_2 composites with different contents of ND_{ox}, under near-UV/Vis light irradiation.

As shown in Figures 4a-c, all the prepared composites led to higher rate constants for DP degradation with respect to that obtained in non-catalytic conditions (photolysis). Regarding the composites prepared without previous oxidation treatment of the carbon material, higher rate constants were obtained when the content of MDs (Figure 4a) or NDs (Figure 4b) was increased from 4 to 15 wt.% (i.e. k increased from 6.7×10^{-3} to 31×10^{-3} min^{-1} for MDT and from 11.8×10^{-3} to 56×10^{-3} min^{-1} for NDT, respectively), the composites with a content of diamond particles higher than 10 wt.% exhibiting always better performance than the bare TiO_2 material (16.3×10^{-3} min^{-1}). These results indicate a marked influence of the diamond powder content on the photocatalytic activity of the composites.

In addition, the composites synthesized with NDs (Figure 4b) were more efficient for DP degradation than those prepared with MDs (Figure 4a) at the same carbon content (i.e. k = 56×10^{-3} and 31×10^{-3} min^{-1} for NDT-15 and MDT-15, respectively, in Table 4). The better performance can be attributed to the size of the TiO_2-NDs composite particles that are smaller and seem to be more homogeneously distributed than the TiO_2-MDs composite particles. It is also noticed that, among the composites prepared with non-oxidized MDs and NDs, the composite containing 15 wt.% of NDs exhibited the best performance (k = 56×10^{-3} min^{-1}) with a complete conversion of DP at the end of 60 min of irradiation.

The introduction of surface functional groups on the nano-sized diamond particles plays an important role in the photocatalytic activity of the composites (Figure 4c and Table 4), the respective pseudo-first order rate constants increasing from 56×10^{-3} to 91×10^{-3} min^{-1} for NDT-15 and ND_{ox}T-15, respectively, and even exceeding the activity obtained for P25 (k = 79×10^{-3} min^{-1}). An increase in the DP mineralization after 60 min was also observed for ND_{ox}T-15, producing a total organic carbon (TOC) reduction of around 45% (similar to that obtained with P25) while for NDT-15 the TOC reduction was 32%.

Table 4. Pseudo-first order rate constant (k) of DP degradation and respective regression coefficient (r^2) when using composites prepared with MDs (MDT), non-oxidized NDs (NDT) and oxidized NDs (ND_{ox}T). Results obtained with Bare-TiO_2, P25 and non-catalytic (photolysis) experiments are also presented.

Catalyst	k (10^{-3} min^{-1})	r^2
MDT-4	6.7 ± 0.5	0.98
MDT-8	17.2 ± 0.9	0.995
MDT-10	20.8 ± 0.2	0.999
MDT-15	31 ± 3	0.98
NDT-4	11.8 ± 0.5	0.995
NDT-8	19.5 ± 0.3	0.9995
NDT-10	35.1 ± 0.4	0.9998
NDT-15	56 ± 2	0.998
ND_{ox}T-6	19 ± 1	0.996
ND_{ox}T-15	91 ± 7	0.997
ND_{ox}T-22	73 ± 3	0.98
ND_{ox}T-37	48 ± 2	0.99
Bare-TiO_2	16.3 ± 0.8	0.994
P25	79 ± 4	0.998
MDs	1.30 ± 0.04	0.991
NDs	1.53 ± 0.07	0.999
ND_{ox}	2.3 ± 0.4	0.991
Photolysis	1.00 ± 0.07	0.98

It is important to refer that the oxidation treatment in air at 703 K produces not only oxygen-containing surface species but also it is known to purify the nanodiamond powders (i.e. eliminating non-diamond carbon in the detonation product by a selective oxidation).[2b, 16] Therefore, the marked enhancement on the photodegradation rate for the ND_{ox}T-15 could be attributed to the significant amount of oxygen surface species on ND_{ox} (mainly carboxylic anhydrides, lactones, phenols and, to a lower extent, carbonyl/quinone groups), which are known to be beneficial for the preparation of TiO_2 nanostructured carbon composites,[7, 9b, 17] and to the increased purity of the nano-sized diamond constituent after the oxidation treatment. In fact, the composite prepared with 15 wt.% of ND_{ox} was the most active among all tested ND_{ox}T materials (Figure 4c) containing lower (6 wt.%) and higher (22 and 37 wt.%) carbon content.

Therefore, the results obtained in this work indicate that nano-sized diamonds can be used in combination with TiO_2 in photocatalytic applications. These composite materials can now be optimized (for instance with respect to their textural characteristics) and tested on adequate substrates, aiming at further technological applications.

Conclusions

Diamond-TiO_2 nanoparticle composites prepared with NDs are more active than those prepared with MDs at comparable carbon contents.

In addition, the oxidation treatment of NDs in air at 703 K produced a powder material (ND_{ox}) with a large content of oxygenated surface groups (mainly carboxylic anhydrides, lactones, phenols and, to a lower extent, carbonyl/quinone groups). The photocatalytic efficiency of these composites is strongly influenced by the diamond content, the composite prepared with the 15 wt.% of ND_{ox} presenting the highest photocatalytic activity for DP degradation, in comparison to the other composites prepared with lower or higher carbon contents.

This work opens a new possibility in the synthesis of TiO_2-nanodiamond composites and promotes their use in heterogeneous photocatalysis.

Experimental Section

Catalyst synthesis

MDs (Technodiamant, The Netherlands) were obtained by extraction from rock samples by drill core or outcrop of about 25 to 100 kg, which were crushed and dissolved in acid or a hot caustic solution.[12] NDs (<10 nm, Sigma Aldrich) were produced by detonating carbon-containing explosives in a closed chamber and immediately cooled at a rate ≥ 3000 K min^{-1}, as described elsewhere.[16] NDs were oxidized (ND_{ox}) by using an environmentally friendly and low cost technique, namely by heating in an open air oven at 703 K for several hours.[18] Composites were synthesized by using the liquid phase deposition method (LPD), adapted from that used to prepare graphene oxide-TiO_2 composites and described elsewhere.[7] Briefly, ammonium hexafluorotitanate (IV), NH_4TiF_6 (0.1 mol L^{-1}), and boric acid, H_3BO_3 (0.3 mol L^{-1}), were added to dispersions of NDs (or MDs) with different desired loadings of carbon material, and heated at 333 K during 2 h under vigorous stirring. The obtained composites were treated in a furnace with N_2 flow at 473 K and labelled as NDT-X, ND_{ox}T-X and MDT-X, for nano-, oxidized nano- and microdiamonds combined with TiO_2 (T), respectively, where X refers to the content of the carbon phase (up to 37 wt.%). TiO_2 alone was also prepared without addition of either of the diamond powders (Bare-TiO_2) and treated by the same procedure as that used for the composites.

Catalyst characterization

The morphology of the composites was determined by scanning electron microscopy (SEM), coupled with energy dispersive X-ray spectroscopy (EDX) in a FEI Quanta 400FEG ESEM/EDAX Genesis X4M instrument, as referred elsewhere.[7] Textural characterization of the samples was carried out by N_2 adsorption-desorption at 77 K with a Quantachrome NOVA 4200e apparatus. The Brunauer-Emmett-Teller (BET) equation was applied to determine the apparent surface area (S_{BET}).[19] The Barrett-Joyner-Halenda (BJH) method was used to determine the pore size distribution.[20] This method was only applied for comparison between the samples and taking into account that its application is more appropriate for adsorption isotherms of type-IV according to IUPAC classification.[21] The surface chemistry of the materials was characterized by temperature programmed desorption (TPD), following a methodology described elsewhere.[14] The contents (in wt.%) of MDs and NDs in the composites were determined by thermogravimetric (TG) analysis using a STA 490 PC/4/H Luxx Netzsch thermal analyser and by heating the sample in air flow from 323 to 1273 K at 20 K min^{-1}.

Photocatalytic experiments

The photocatalytic efficiencies of the materials were evaluated for degradation of a 100 mg L^{-1} DP (3.40×10^{-4} mol L^{-1}) aqueous solution under near-UV/Vis irradiation, the experimental system described in detail elsewhere.[7] The irradiation source consisted in a Heraeus TQ 150 medium-pressure mercury vapour lamp. A DURAN® glass cooling jacket was used for obtaining irradiation in the near-UV to visible light range (λ > 350 nm). The photon flow entering the reactor was determined with an Ocean Optics spectroradiometer positioned in the photoreactor, i.e. 4 cm away from the lamp, the total irradiance at this point being equal to 27 mW cm^{-2}, while the irradiance determined by actinometry (near the lamp) was ca. 50 mW cm^{-2}. The concentration of DP was determined by High Performance Liquid Chromatography (HPLC) with a Hitachi Elite LaChrom system equipped with a Hydrosphere C18 column. The total organic carbon (TOC) was also determined for selected samples using a Shimadzu TOC-5000A analyzer.

Acknowledgements

Financial support for this work was provided by projects PTDC/AAC-AMB/122312/2010 and PEst-C/EQB/LA0020/2011 financed by FEDER through COMPETE and by Fundação para a Ciência e a Tecnologia (FCT). LMPM and SMT acknowledge financial support from FCT grants SFRH/BPD/88964/2012 and SFRH/BPD/74239/2010, respectively. SACC also acknowledges financial support from FCT (CIENCIA 2007 program). JGB acknowledges Houcine Dhieb for technical assistance and the Executive Research Agency of the European Union for funding under the Marie Curie grant NANODIA (272448).

Keywords: nanodiamonds • microdiamonds • titanium dioxide • heterogeneous photocatalysis • water pollutants

[1] O. A. Shenderova, V. V. Zhirnov, D. W. Brenner, *Critical Reviews in Solid State and Materials Sciences* **2002**, *27*, 227-356.

[2] a) M. Ozawa, M. Inaguma, M. Takahashi, F. Kataoka, A. Krüger, E. Ōsawa, *Advanced Materials* **2007**, *19*, 1201-1206; b) V. N. Mochalin, O. Shenderova, D. Ho, Y. Gogotsi, *Nature Nanotechology* **2012**, *7*, 11-23.

[3] J. Zhang , D. S. Su , R. Blume, R. Schlögl, R. Wang, X. Yang, A. Gajović, *Angewandte Chemie International Edition* **2010**, *49*, 8640-8644.

[4] V. N. Mochalin, I. Neitzel, B. J. M. Etzold, A. Peterson, G. Palmese, Y. Gogotsi, *ACS Nano* **2011**, *5*, 7494-7502.

[5] J. R. Maze, P. L. Stanwix, J. S. Hodges, S. Hong, J. M. Taylor, P. Cappellaro, L. Jiang, M. V. G. Dutt, E. Togan, A. S. Zibrov, A. Yacoby, R. L. Walsworth, M. D. Lukin, *Nature* **2008**, *455*, 644-647.

[6] a) A. L. Linsebigler, G. Lu, J. T. Yates, *Chemical Reviews* **1995**, *95*, 735-758; b) A. Fujishima, K. Honda, *Nature* **1972**, *238*, 37-38; c) S. C. Roy, O. K. Varghese, M. Paulose, C. A. Grimes, *ACS Nano* **2010**, *4*, 1259-1278.

[7] L. M. Pastrana-Martínez, S. Morales-Torres, V. Likodimos, J. L. Figueiredo, J. L. Faria, P. Falaras, A. M. T. Silva, *Applied Catalysis B: Environmental* **2012**, *123–124*, 241-256.

[8] a) H. Zhang, X. Lv, Y. Li, Y. Wang, J. Li, *ACS Nano* **2009**, *4*, 380-386; b) S. Morales-Torres, L. Pastrana-Martínez, J. Figueiredo, J. Faria, A. T. Silva, *Environmental Science and Pollution Research* **2012**, *19*, 3676-3687.

[9] a) W. Wang, P. Serp, P. Kalck, C. G. Silva, J. L. Faria, *Materials Research Bulletin* **2008**, *43*, 958-967; b) R. R. N. Marques, M. J. Sampaio, P. M. Carrapiço, C. G. Silva, S. Morales-Torres, G. Dražić, J. L. Faria, A. M. T. Silva, *Catalysis Today*, in press; c) M. J. Sampaio, C. G. Silva, R. R. N. Marques, A. M. T. Silva, J. L. Faria, *Catalysis Today* **2011**, *161*, 91-96.

[10] R. Leary, A. Westwood, *Carbon* **2011**, *49*, 741-772.

[11] K.-D. Kim, N. K. Dey, H. O. Seo, Y. D. Kim, D. C. Lim, M. Lee, *Applied Catalysis A: General* **2011**, *408*, 148-155.

[12] S. A. C. Carabineiro, M. Avalos-Borja, J. G. Buijnsters, in *Current microscopy contributions to advances in science and technology, Vol. 2* (Ed.: A. Méndez-Vilas), Formatex Microscopy Book series, Formatex Research Center, Badajoz, Spain, **2012**, pp. 1246-1251.

[13] K. D. Behler, A. Stravato, V. Mochalin, G. Korneva, G. Yushin, Y. Gogotsi, *ACS Nano* **2009**, *3*, 363-369.

[14] a) J. L. Figueiredo, M. F. R. Pereira, M. M. A. Freitas, J. J. M. Órfão, *Industrial & Engineering Chemistry Research* **2007**, *46*, 4110-4115; b) J. L. Figueiredo, M. F. R. Pereira, M. M. A. Freitas, J. J. M. Órfão, *Carbon* **1999**, *37*, 1379-1389.

[15] S. Morales-Torres, F. J. Maldonado-Hódar, A. F. Pérez-Cadenas, F. Carrasco-Marín, *Journal of Hazardous Materials* **2010**, *183*, 814-822.

[16] A. M. Schrand, S. A. C. Hens, O. A. Shenderova, *Critical Reviews in Solid State and Materials Sciences* **2009**, *34*, 18-74.

[17] C. G. Silva, J. L. Faria, *Applied Catalysis B: Environmental* **2010**, *101*, 81-89.

[18] a) S. Osswald, G. Yushin, V. Mochalin, S. O. Kucheyev, Y. Gogotsi, *Journal of the American Chemical Society* **2006**, *128*, 11635-11642; b) O. Shenderova, A. Koscheev, N. Zaripov, I. Petrov, Y. Skryabin, P. Detkov, S. Turner, G. Van Tendeloo, *The Journal of Physical Chemistry C* **2011**, *115*, 9827-9837.

[19] S. Brunauer, P. H. Emmett, E. Teller, *Journal of the American Chemical Society* **1938**, *60*, 309-319.

[20] E. P. Barrett, L. G. Joyner, P. P. Halenda, *Journal of the American Chemical Society* **1951**, *73*, 373-380.

[21] R. C. Bansal, J. B. Donnet, F. Stoeckli, *Active Carbon*, Marcel Dekker, New York, **1988**.

Received: ((will be filled in by the editorial staff))
Published online: ((will be filled in by the editorial staff))

FULL PAPER

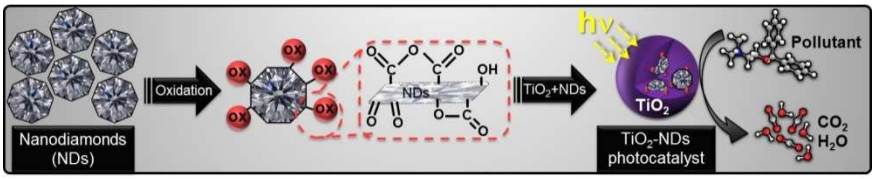

Nanodiamonds in photocatalysis: Nanodiamond-TiO_2 composites have been synthesized and used, for the first time, in the photocatalytic treatment of water pollutants. A significant enhancement in the photocatalytic performance was observed when the nanodiamonds were oxidized, containing mainly carboxylic anhydrides, lactones, phenols and carbonyl/quinone groups on their surface.

*Luisa M. Pastrana-Martínez, Sergio Morales-Torres, Sónia A.C. Carabineiro, Josephus G. Buijnsters, Joaquim L. Faria, José L. Figueiredo, Adrián M.T. Silva**

Page No. – Page No.

Nanodiamond-TiO_2 composites for heterogeneous photocatalysis